

seems to be characteristic of this type of photooxidation.²⁷ It may reflect the participation of higher vibrational levels of a single excited state. In addition or as an alternative, more than one internal excited state of the cluster may be involved. The electron transfer from higher energy excited states could become more efficient due to an increase of the redox potentials.

Acknowledgment. Financial support for the research by the Deutsche Forschungsgemeinschaft and the Fonds der Chemischen Industrie is gratefully acknowledged.

Registry No. [Ta₆Br₁₂]²⁺, 12343-63-4; [Ta₆Br₁₂]³⁺, 12343-64-5; H₂, 1333-74-0; HCl, 7647-01-0; H₂O, 7732-18-5.

Contribution from the Istituto di Chimica Generale dell'Università di Milano, 20133 Milano, Italy, Centro del CNR per lo studio della sintesi e della struttura dei composti dei metalli di transizione, 20133 Milano, Italy, and Chemistry Department, Brookhaven National Laboratory, Upton, New York 11973

Synthesis of Bimetallic Fe-Ni Carbonyl Clusters: Crystal Structure of [N(CH₃)₃CH₂Ph][Fe₃Ni(CO)₈(μ-CO)₄(μ₃-H)]

ALESSANDRO CERIOTTI,^{1a} PAOLO CHINI,[†] ALESSANDRO FUMAGALLI,^{1b,c} THOMAS F. KOETZLE,^{*1c} GIULIANO LONGONI,^{*1b} and FUSAO TAKUSAGAWA^{1c,d}

Received December 29, 1982

Redox condensation of [Fe₃(CO)₁₁]²⁻ with Ni(CO)₄ in tetrahydrofuran affords the tetranuclear dianion [Fe₃Ni(CO)₁₂]²⁻. Subsequent protonation with acids results in formation of the corresponding [Fe₃Ni(CO)₁₂H]⁻ anion. This monoanionic species has also been obtained by reaction of [Fe₃(CO)₁₁]²⁻ with NiCl₂·xEtOH. Both Fe₃Ni systems have been isolated in the solid state in high yield with a variety of tetrasubstituted ammonium and phosphonium salts. An X-ray diffraction study of the trimethylbenzylammonium salt of [Fe₃Ni(CO)₁₂H]⁻ reveals a structure with a tetrahedron of metal atoms surrounded by eight terminal and four edge-bridging carbonyl groups. The hydride ligand has been located over the center of an Fe₂Ni face at a distance of 0.60 (3) Å from the trimetal plane. The corresponding [Fe₃Ni(CO)₁₂]²⁻ dianion is suggested to possess an analogous structure on the basis of its IR spectrum. Crystallographic data for [C₁₀H₁₆N]⁺[C₁₂HFe₃NiO₁₂]⁻: fw 713.64, triclinic, space group P $\bar{1}$, Z = 2, a = 7.416 (1) Å, b = 13.849 (2) Å, c = 14.108 (2) Å, α = 103.13 (2)°, β = 103.15 (2)°, γ = 99.23 (2)°, R(F²) = 0.030 for 3860 reflections measured at room temperature.

Introduction

Nickel subgroup metals show significant differences in their homometallic carbonyl cluster chemistry.² A first contact point between nickel and platinum has been established with the synthesis of isoelectronic [M₆(CO)₆(μ-CO)₆]²⁻ and [M₉(CO)₉(μ-CO)₉]²⁻ (M = Ni, Pt) dianions, although the nickel derivatives are not isostructural with the platinum ones.³⁻⁵ The recent characterization of a series of bimetallic Fe-Pd and Fe-Pt carbonyl clusters has suggested that the fact that the corresponding palladium carbonyl clusters do not exist may probably be ascribed to intrinsic weakness of the Pd-CO bond, at least where low-nuclearity clusters are concerned.^{6,7} The isolation of isostructural [Fe₃M(CO)₁₆]²⁻ (M = Pd, Pt) species during that work prompted us to investigate the chemistry of the analogous bimetallic Fe-Ni carbonyl compounds.

Experimental Section

All reactions were performed under pure nitrogen or carbon monoxide in freshly distilled and dried solvents. IR spectra were recorded on a Perkin-Elmer 457 grating spectrophotometer using calcium fluoride cells. Analytical data were obtained as described elsewhere.⁸ NMR spectra were recorded on a Varian XL-100 instrument. The [Fe₃(CO)₁₁]²⁻ and NiCl₂·xEtOH starting materials were prepared by following methods previously given in the literature.⁸

Synthesis of [PPh₃(CH₂Ph)]₂[Fe₃Ni(CO)₁₂]. [PPh₃(CH₂Ph)]₂[Fe₃(CO)₁₁]²⁻ (2.23 g) and Ni(CO)₄ (1 mL) were dissolved in anhydrous THF (25 mL) in a 100-mL, two-necked, round-bottomed flask equipped with a condenser cooled to about -30 °C. The solution was stirred at room temperature, while the evolving carbon monoxide was continuously removed with a slow stream of nitrogen. After 6 h of stirring, the resulting brown solution was evaporated to dryness. The residue was dissolved in acetone (20 mL), the mixture filtered, and the product precipitated by slow diffusion of 2-propanol (40 mL). After a week, well-shaped crystals of [PPh₃(CH₂Ph)]₂[Fe₃Ni(CO)₁₂] (2.01 g, 84% yield) were isolated by filtration and dried under vacuum. Anal. Calcd: [PPh₃(CH₂Ph)]⁺, 55.66; Fe, 13.21; Ni, 4.63; CO, 26.49;

[PPh₃(CH₂Ph)]⁺:Fe:Ni:CO = 2:3:1:12. Found: [PPh₃(CH₂Ph)]⁺, 55.68; Fe, 13.03; Ni, 4.57; CO, 26.11; [PPh₃(CH₂Ph)]⁺:Fe:Ni:CO = 2.03:2.99:1.00:12.16.

The tetra-*n*-butyl- and trimethylbenzylammonium salts of [Fe₃Ni(CO)₁₂]²⁻ were analogously synthesized from the corresponding [Fe₃(CO)₁₁]²⁻ salts and isolated. All these salts are readily soluble in polar solvents such as THF, acetone, acetonitrile, and dimethyl sulfoxide (Me₂SO), less soluble in alcohols, and insoluble in apolar solvents such as toluene or heptane.

Synthesis of [PPh₃(CH₂Ph)][Fe₃Ni(CO)₁₂H] from [Fe₃Ni(CO)₁₂]²⁻. [PPh₃(CH₂Ph)]₂[Fe₃Ni(CO)₁₂] (1.07 g) was dissolved in THF (25 mL) under nitrogen atmosphere in a 100-mL Schlenk tube. Upon dropwise addition of 48% H₃PO₄ (0.3 mL), the stirred dark brown solution turned rapidly green, and the IR spectrum of the solution showed the complete disappearance of absorptions due to the dianion and the appearance of the absorptions due to the corresponding [Fe₃Ni(CO)₁₂H]⁻ derivative. The solution was evaporated to dryness under vacuum and the residue suspended in methanol (25 mL). The precipitation of [PPh₃(CH₂Ph)][Fe₃Ni(CO)₁₂H] was completed by addition of an excess of triphenylbenzylphosphonium chloride (0.5 g) and water (20 mL) with stirring. The resulting microcrystalline precipitate was filtered under nitrogen, washed with a mixture of

- (1) (a) Istituto di Chimica Generale dell'Università di Milano. (b) Centro del CNR per lo studio della sintesi e della struttura dei composti dei metalli di transizione. (c) Brookhaven National Laboratory. (d) Present address: Institute for Cancer Research, Philadelphia, PA 19111.
- (2) Chini, P.; Longoni, G.; Albano, V. G. *Adv. Organomet. Chem.* **1976**, *14*, 285.
- (3) Calabrese, J. C.; Dahl, L. F.; Chini, P.; Longoni, G.; Martinengo, S. J. *Am. Chem. Soc.* **1974**, *96*, 2614.
- (4) Calabrese, J. C.; Dahl, L. F.; Cavalieri, A.; Chini, P.; Longoni, G.; Martinengo, S. J. *Am. Chem. Soc.* **1974**, *96*, 2616.
- (5) Lower, L. D. Ph.D. Thesis, University of Wisconsin, Madison, 1976. Dahl, L. F., personal communication.
- (6) Longoni, G.; Manassero, M.; Sansoni, M. *J. Am. Chem. Soc.* **1980**, *102*, 3242.
- (7) Longoni, G.; Manassero, M.; Sansoni, M. *J. Am. Chem. Soc.* **1980**, *102*, 7973.
- (8) (a) Longoni, G.; Chini, P.; Cavalieri, A. *Inorg. Chem.* **1976**, *15*, 3025. Yip-Kwai Lo, F.; Longoni, G.; Chini, P.; Lower, L. D.; Dahl, L. F. *J. Am. Chem. Soc.* **1980**, *102*, 7691 and references therein.

[†] Deceased.

methanol and water (1:2), and dried under vacuum. The compound was recrystallized from acetone (20 mL) by means of slow diffusion of 2-propanol (40 mL); yield 0.63 g, 82%. Anal. Calcd: $[\text{PPh}_3(\text{CH}_2\text{Ph})]^+$, 38.52; Fe, 18.28; Ni, 6.4; CO, 36.67; $[\text{PPh}_3(\text{CH}_2\text{Ph})]^+ \cdot \text{Fe} \cdot \text{Ni} \cdot \text{CO} \cdot \text{H} = 1:3:1:12:1$. Found: $[\text{PPh}_3(\text{CH}_2\text{Ph})]^+$, 38.00; Fe, 17.98; Ni, 6.49; CO, 36.01; $[\text{PPh}_3(\text{CH}_2\text{Ph})]^+ \cdot \text{Fe} \cdot \text{Ni} \cdot \text{CO} \cdot \text{H} = 1.00:2.99:1.03:11.95:0.80$ (by integration of the ^1H NMR signal at $\delta -20.5$ against the CH_2 signal of the cation).

The tetra-*n*-butyl- and trimethylbenzylammonium, as well as the bis(triphenylphosphine)nitrogen(1+) (PPN) salts, were analogously obtained by starting from the corresponding $[\text{Fe}_3\text{Ni}(\text{CO})_{12}]^{2-}$ salts. All these compounds are readily soluble in THF, acetone, and acetonitrile, less soluble in methanol, and sparingly soluble or insoluble in 2-propanol, toluene, and heptane. They have been crystallized by slow diffusion from acetone-2-propanol or THF-heptane.

Synthesis of $[\text{N}(\text{C}_4\text{H}_9)_4][\text{Fe}_3\text{Ni}(\text{CO})_{12}\text{H}]$ from $[\text{Fe}_3(\text{CO})_{11}]^{2-}$ and $\text{NiCl}_2 \cdot x\text{EtOH}$. $[\text{N}(\text{C}_4\text{H}_9)_4][\text{Fe}_3(\text{CO})_{11}]$ (1.42 g) was dissolved in THF (20 mL) in a 100-mL, round-bottomed, two-necked flask equipped with a microburet. A 0.65 M solution of $\text{NiCl}_2 \cdot x\text{EtOH}$ in ethanol (8 mL) was added with stirring over a 2-h period. After addition of ca. 2 mL, the originally dark red solution turned brown, and the IR spectrum showed absorptions due to $[\text{Fe}_3\text{Ni}(\text{CO})_{12}]^{2-}$. Upon addition of the remaining $\text{NiCl}_2 \cdot x\text{EtOH}$ solution the absorptions of the dianion slowly disappeared and were replaced by those of the $[\text{Fe}_3\text{Ni}(\text{CO})_{12}\text{H}]^-$, while the color of the solution turned dark green. The resulting suspension was filtered and evaporated to dryness under vacuum, and the residue was suspended in methanol (25 mL). The precipitation of $[\text{N}(\text{C}_4\text{H}_9)_4][\text{Fe}_3\text{Ni}(\text{CO})_{12}\text{H}]$ was completed by adding tetra-*n*-butylammonium chloride (0.5 g) and water (20 mL) with stirring. The resulting microcrystalline precipitate was filtered out, washed with a mixture of methanol and water (2:1), and dried under vacuum. The compound was purified by dissolving it in acetone, followed by filtration and precipitation by slow diffusion of 2-propanol; yield 0.84 g, 71%. With use of the above procedure starting with an equimolecular amount of $[\text{N}(\text{C}_4\text{H}_9)_4][\text{Fe}_2(\text{CO})_8]$, instead of $[\text{N}(\text{C}_4\text{H}_9)_4][\text{Fe}_3(\text{CO})_{11}]$, a similar course of the reaction was observed.

Reaction of $[\text{Fe}_3\text{Ni}(\text{CO})_{12}]^{2-}$ with CO. $[\text{N}(\text{C}_4\text{H}_9)_4][\text{Fe}_3\text{Ni}(\text{CO})_{12}]$ (0.51 g) was dissolved in THF (20 mL), and the mixture was stirred under 1 atm of carbon monoxide at room temperature. IR monitoring of the stirred solution showed the rapid formation of $\text{Ni}(\text{CO})_4$ and $[\text{Fe}_3(\text{CO})_{11}]^{2-}$. After 6 h of stirring, IR spectroscopy indicated that $[\text{Fe}_3(\text{CO})_{11}]^{2-}$ was completely degraded to a mixture of $\text{Fe}(\text{CO})_5$, $[\text{Fe}_2(\text{CO})_8]^{2-}$, and $[\text{Fe}(\text{CO})_4\text{H}]^-$.

Reaction of $[\text{Fe}_3\text{Ni}(\text{CO})_{12}\text{H}]^-$ with CO. $[\text{PPN}][\text{Fe}_3\text{Ni}(\text{CO})_{12}\text{H}]$ (0.67 g) was dissolved in acetonitrile (20 mL), and the mixture was stirred under carbon monoxide at room temperature. The initially green-brown solution rapidly turned red-violet, and after 2 h of stirring, IR monitoring showed the complete replacement of the absorptions due to $[\text{Fe}_3\text{Ni}(\text{CO})_{12}\text{H}]^-$ with those of $\text{Ni}(\text{CO})_4$ (2040 cm^{-1}) and $[\text{Fe}_3(\text{CO})_{11}\text{H}]^-$ (1995 (s), 1970 (ms), 1940 (sh), 1740 (w) cm^{-1}). The solution was evaporated to dryness to eliminate $\text{Ni}(\text{CO})_4$, and the residue dissolved in acetone- d_6 showed an NMR signal at τ 25.1, as expected for a sample of $[\text{Fe}_3(\text{CO})_{11}\text{H}]^-$.

Reaction of $[\text{Fe}(\text{CO})_4]^{2-}$ with $\text{Ni}(\text{CO})_4$. A sample of $[\text{Na}(\text{THF})_2][\text{Fe}(\text{CO})_4]$ (1.6 g; $x \approx 4$) was suspended in anhydrous THF (25 mL), and an excess of $\text{Ni}(\text{CO})_4$ (4.5 mL) was added. After 72 h of stirring at room temperature, solid unreacted $[\text{Na}(\text{THF})_2][\text{Fe}(\text{CO})_4]$ was still present while the solution was deep red-orange. The suspension was filtered and the resulting clear solution evaporated under vacuum to eliminate the unreacted $\text{Ni}(\text{CO})_4$. A sample of the residue dissolved in THF showed a complicated pattern with the main absorptions at 1955, 1915, 1875, 1850, and 1830 cm^{-1} , indicating the presence in solution of a mixture of compounds. The entire residue was therefore dissolved in methanol (30 mL) and subjected to fractional precipitation by adding (a) a solution of $[\text{N}(\text{CH}_3)_3(\text{CH}_2\text{Ph})]\text{Cl}$ (1 g) in methanol (10 mL), (b) solid $[\text{N}(\text{CH}_3)_3(\text{CH}_2\text{Ph})]\text{Cl}$ (ca. 2 g), (c) water (20 mL), and (d) finally 1 mL of H_3PO_4 .

Fraction (a) + (b) consisted mainly of $[\text{Fe}_3\text{Ni}(\text{CO})_{12}]^{2-}$ with $[\text{Fe}(\text{CO})_4\text{H}]^-$ and $[\text{Fe}_2(\text{CO})_8]^{2-}$ impurities, as shown by IR and NMR spectroscopy and subsequent workup.

Fraction d initially gave a red oil that crystallized on standing overnight to yield a pure sample of $[\text{Fe}_3\text{Ni}(\text{CO})_{12}\text{H}]^-$. By contrast, fraction c showed IR absorptions at 1960 (s), 1930 (m), 1910 (m), 1885 (w), and 1830 (s, br) cm^{-1} , which could not be attributed to any known Fe, Ni, or bimetallic Fe-Ni clusters or mixtures of the above.

Table I. Summary of Crystal Data and Refinement Results for $[\text{N}(\text{CH}_3)_3(\text{CH}_2\text{Ph})][\text{Fe}_3\text{Ni}(\text{CO})_{12}\text{H}]$

space group: $P\bar{1}$	$a = 7.416$ (1) Å	$\alpha = 103.13$ (2)°
$Z = 2$	$b = 13.849$ (2) Å	$\beta = 103.15$ (2)°
fw = 713.64	$c = 14.108$ (2) Å	$\gamma = 99.23$ (2)°
$\rho(\text{calcd}) = 1.77$ g cm^{-3}		
total no. of refls measd	5961	
no. of unique refls used in the structure analysis (m)	3860	
no. of variable parameters (n)	421	
agreement among equiv refls	$R = \sum(\sum_i F_i - F_o ^2) / \sum_i F_o ^2 = 0.010$	
final agreement factors	$R(F^2) = \sum F_o ^2 - k^2 F_c^2 / \sum F_o ^2 = 0.030$	
	$R_w(F^2) = [\sum w(F_o^2 - k^2 F_c^2)^2 / \sum w F_o^4]^{1/2} = 0.032$	
	$S = [\sum w(F_o^2 - k^2 F_c^2)^2 / (m - n)]^{1/2} = 1.167$	

Attempts to crystallize this material have so far been unsuccessful. Similar results have also been obtained for the reaction of $[\text{N}(\text{C}_4\text{H}_9)_4][\text{Fe}_2(\text{CO})_8]$ with $\text{Ni}(\text{CO})_4$ in excess.

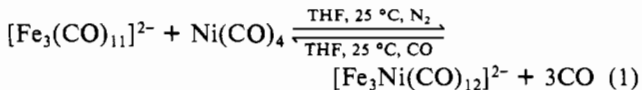
X-ray Diffraction Analysis of $[\text{N}(\text{CH}_3)_3(\text{CH}_2\text{Ph})][\text{Fe}_3\text{Ni}(\text{CO})_{12}\text{H}]$. A dark green prismatic crystal of $[\text{N}(\text{CH}_3)_3(\text{CH}_2\text{Ph})][\text{Fe}_3\text{Ni}(\text{CO})_{12}\text{H}]$ with approximate dimensions $0.02 \times 0.03 \times 0.05$ cm was sealed in a quartz capillary under nitrogen and used for X-ray diffraction measurements. Unit cell parameters and other crystallographic details are given in Table I. A full hemisphere of reciprocal space up to $2\theta = 55^\circ$, and a second hemisphere up to $2\theta = 30^\circ$ were sampled at room temperature. A total of 5961 reflections was measured on an Enraf-Nonius CAD-4 diffractometer, with a θ - 2θ scan mode and graphite-monochromatized Mo K α radiation ($\lambda = 0.71069$ Å). Three monitor reflections were measured at 50 reflection intervals and exhibited a limited decay in intensity of no more than 9% during the data collection. Integrated raw intensities were corrected for Lorentz, polarization, absorption ($\mu = 23.9$ cm^{-1} , calculated⁹ transmission range 0.84–0.93), and decay effects and merged to give 3860 independent reflections having $F_o^2 > \sigma(F_o^2)$.

The structure was solved by standard heavy-atom techniques, and all non-hydrogen atoms were refined¹⁰ with anisotropic thermal factors. Initially the four metals were treated as iron atoms, and the position of the unique nickel atom was subsequently assigned by considering the individual thermal parameters. The agreement factor $R_w(F^2)$ decreased by 0.009 when the nickel atom was properly positioned,^{11,12} and the assignment has been confirmed by the final stereochemistry.

All hydrogen atoms including the hydride ligand were located in difference Fourier maps and were included in the final refinement with isotropic thermal parameters. The quantity minimized was $\sum w(F_o^2 - k^2 F_c^2)^2$ with weights w chosen as $w = (\sigma_{\text{count}}^2(F_o^2) + (0.02F_o^2)^2)^{-1}$. Several cycles of full-matrix refinement resulted in the final agreement factors of $R(F^2) = 0.030$ and $R_w(F^2) = 0.032$. Atomic coordinates are reported in Table II, while thermal parameters (Table I-S) and a list of F^2 values are available as supplementary material.

Results and Discussion

Synthesis and Chemical Characterization of $[\text{Fe}_3\text{Ni}(\text{CO})_{12}]^{2-}$ and $[\text{Fe}_3\text{Ni}(\text{CO})_{12}\text{H}]^-$. When $[\text{Fe}_3(\text{CO})_{11}]^{2-}$ and $\text{Ni}(\text{CO})_4$ are mixed in THF, a smooth redox condensation reaction² occurs, according to equilibrium 1. Under a nitrogen atmosphere at



(9) North, A. C. T.; Phillips, D. C.; Mathews, F. S. *Acta Crystallogr., Sect. A* 1968, A24, 351.

(10) Least-squares calculations were carried out with a modified version of the program ORFLS: Busing, W. R.; Martin, K. O.; Levy, H. A. Report ORNL-TM-305; Oak Ridge National Laboratory: Oak Ridge, TN, 1962.

(11) This represents a significant improvement in fit, according to the criteria set forth by: Hamilton, W. C. *Acta Crystallogr.* 1965, 18, 502.

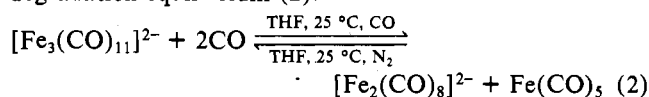
(12) Scattering factors were those for neutral atoms given in: "International Tables for X-ray Crystallography"; Kynoch Press: Birmingham, England, 1975; Vol IV (including anomalous dispersion corrections for metal atoms).

Table II. Fractional Atomic Coordinates

atom	x	y	z
Ni	0.10103 (4)	0.15132 (2)	0.35599 (2)
Fe(1)	-0.01069 (4)	0.15969 (2)	0.17974 (2)
Fe(2)	0.11479 (4)	0.32357 (2)	0.32624 (2)
Fe(3)	-0.21645 (4)	0.19934 (2)	0.31511 (2)
O(1)	0.3828 (3)	0.0662 (1)	0.4660 (1)
O(2)	-0.3519 (2)	0.1010 (1)	0.0105 (1)
O(3)	0.2291 (3)	0.1152 (1)	0.0454 (1)
O(4)	-0.0549 (2)	0.4977 (1)	0.3742 (1)
O(5)	0.4728 (2)	0.4539 (1)	0.3380 (2)
O(6)	-0.4069 (2)	0.3038 (1)	0.1764 (1)
O(7)	-0.5262 (2)	0.0187 (1)	0.2322 (1)
O(8)	-0.3262 (3)	0.3164 (1)	0.4854 (1)
O(12)	-0.0127 (2)	0.3530 (1)	0.1216 (1)
O(14)	-0.0598 (3)	-0.0502 (1)	0.2015 (1)
O(24)	0.2579 (3)	0.3320 (1)	0.5421 (1)
O(34)	-0.1231 (3)	0.0971 (2)	0.4806 (2)
C(1)	0.2703 (3)	0.0969 (2)	0.4223 (2)
C(2)	-0.2202 (3)	0.1229 (2)	0.0785 (2)
C(3)	0.1379 (3)	0.1336 (2)	0.0989 (2)
C(4)	0.0065 (3)	0.4274 (2)	0.3563 (2)
C(5)	0.3350 (3)	0.4008 (2)	0.3322 (2)
C(6)	-0.3250 (3)	0.2643 (2)	0.2293 (2)
C(7)	-0.4043 (3)	0.0892 (2)	0.2640 (2)
C(8)	-0.2819 (3)	0.2720 (2)	0.4190 (2)
C(12)	0.0121 (3)	0.3040 (2)	0.1791 (1)
C(14)	-0.0251 (3)	0.0373 (2)	0.2132 (2)
C(24)	0.1963 (3)	0.3109 (2)	0.4551 (2)
C(34)	-0.0978 (3)	0.1301 (2)	0.4152 (2)
H	0.147 (4)	0.212 (2)	0.281 (2)
N	0.6735 (3)	0.2625 (1)	-0.2362 (1)
C(1')	0.7242 (4)	0.1866 (2)	-0.3153 (2)
C(2')	0.7788 (4)	0.2579 (2)	-0.1333 (2)
C(3')	0.7357 (4)	0.3680 (2)	-0.2473 (2)
C(4')	0.4575 (3)	0.2350 (2)	-0.2519 (2)
C(5')	0.3871 (3)	0.3048 (2)	-0.1783 (2)
C(6')	0.3717 (3)	0.2848 (2)	-0.0873 (2)
C(7')	0.3062 (3)	0.3499 (2)	-0.0203 (2)
C(8')	0.2508 (3)	0.4347 (2)	-0.0427 (2)
C(9')	0.2633 (3)	0.4549 (2)	-0.1338 (2)
C(10')	0.3298 (3)	0.3899 (2)	-0.2016 (2)
H(6)	0.399 (4)	0.224 (2)	-0.070 (2)
H(7)	0.281 (4)	0.334 (2)	0.035 (2)
H(8)	0.204 (4)	0.479 (2)	-0.003 (2)
H(9)	0.246 (4)	0.514 (2)	-0.146 (2)
H(10)	0.340 (4)	0.409 (2)	-0.263 (2)
H(4A)	0.434 (4)	0.170 (2)	-0.247 (2)
H(4B)	0.400 (4)	0.232 (2)	-0.316 (2)
H(1A)	0.699 (4)	0.116 (2)	-0.308 (2)
H(1B)	0.861 (4)	0.205 (2)	-0.307 (2)
H(1C)	0.662 (4)	0.184 (2)	-0.383 (2)
H(2A)	0.765 (3)	0.299 (2)	-0.086 (2)
H(2B)	0.906 (4)	0.273 (2)	-0.129 (2)
H(2C)	0.742 (4)	0.189 (2)	-0.138 (2)
H(3A)	0.690 (4)	0.366 (2)	-0.304 (2)
H(3B)	0.881 (4)	0.380 (2)	-0.245 (2)
H(3C)	0.721 (4)	0.415 (2)	-0.200 (2)

room temperature the reaction corresponding to the right-hand side of equilibrium 1 is generally complete in ca. 6 h. On the contrary, under a carbon monoxide atmosphere (25 °C, 1 atm), the equilibrium (1) is completely shifted to the left, as shown by IR monitoring.

The dark brown $[\text{Fe}_3\text{Ni}(\text{CO})_{12}]^{2-}$ dianion has been obtained in very high yield (ca. 80–90%), and practically pure, by using an excess of $\text{Ni}(\text{CO})_4$ and continuously removing the evolving carbon monoxide from the reaction vessel with a slow stream of nitrogen. A buildup of a carbon monoxide partial pressure in the reaction vessel as the condensation reaction proceeds not only depresses the yield by reversing equilibrium 1 but also results in a less pure final product owing to the concomitant degradation equilibrium (2).



The $[\text{Fe}_3\text{Ni}(\text{CO})_{12}]^{2-}$ dianion has been isolated in the crystalline state with a variety of tetrasubstituted ammonium or phosphonium salts by simply removing the excess $\text{Ni}(\text{CO})_4$ under vacuum and by precipitation with apolar solvents. All these salts are readily soluble in polar solvents such as THF, acetone, and acetonitrile, less soluble in methanol, and sparingly soluble or insoluble in 2-propanol and apolar solvents. In THF the triphenylbenzylphosphonium salt shows IR absorptions in the carbonyl stretching region at 2010 (vw), 1955 (m, sh), 1935 (s), 1905 (mw, sh), 1805 (mw), 1795 (sh) and 1740 (mw) cm^{-1} .

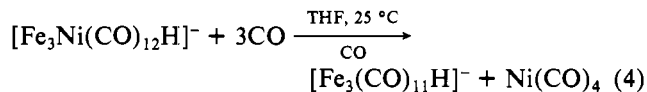
The $[\text{Fe}_3\text{Ni}(\text{CO})_{12}]^{2-}$ dianion is stable in solution under a nitrogen atmosphere, up to ca. 100 °C. Air oxidation is slow, both in the solid state and in solution, and results in complete decomposition. No further reaction of $[\text{Fe}_3\text{Ni}(\text{CO})_{12}]^{2-}$ with excess $\text{Ni}(\text{CO})_4$ has been observed, whereas reaction with excess $\text{Fe}(\text{CO})_5$ at 80 °C results in a mixture of $[\text{Fe}_4(\text{CO})_{13}]^{2-}$, $\text{Ni}(\text{CO})_4$, and an as yet uncharacterized red species that shows its strongest IR absorption at 1970 cm^{-1} .

Upon reaction with aqueous H_3PO_4 (48%) or hydrochloric acid, the brown $[\text{Fe}_3\text{Ni}(\text{CO})_{12}]^{2-}$ dianion is quantitatively converted into the corresponding dark green $[\text{Fe}_3\text{Ni}(\text{CO})_{12}\text{H}]^-$ derivative. The protonation reaction (3) is completely shifted to the right in THF, CH_2Cl_2 , and methanol, but can easily be reversed upon treatment with a base (KOH, $\text{KO}t\text{-Bu}$), or even by dissolution in a strong ionization solvent such as dimethyl sulfoxide (Me_2SO) or dimethylformamide. The



$[\text{Fe}_3\text{Ni}(\text{CO})_{12}\text{H}]^-$ monoanion has been isolated in a crystalline state and in high yield (ca. 80%) with a variety of tetrasubstituted ammonium or phosphonium salts. The triphenylbenzylphosphonium salt in THF shows an IR spectrum similar to that of the parent dianion but shifted to higher frequencies in agreement with the reduced free negative charge (ν_{CO} at 2070 (vw), 2030 (m), 1990 (s), 1965 (mw), 1935 (mw), 1875 (mw), 1830 (w), and 1790 (mw) cm^{-1}). The hydric nature of the proton is confirmed by the presence of a sharp ^1H NMR singlet in acetone- d_6 at δ -20.5.

As is the case for the parent $[\text{Fe}_3\text{Ni}(\text{CO})_{12}]^{2-}$ dianion, $[\text{Fe}_3\text{Ni}(\text{CO})_{12}\text{H}]^-$ is rapidly and irreversibly degraded under a carbon monoxide atmosphere to a mixture of $[\text{Fe}_3(\text{CO})_{11}\text{H}]^-$ and $\text{Ni}(\text{CO})_4$, as shown by IR and ^1H NMR monitoring (reaction 4). Under these experimental conditions,



there is no trace of further degradation of $[\text{Fe}_3(\text{CO})_{11}\text{H}]^-$ by carbon monoxide,¹³ nor is there any evidence for occurrence of the reverse reaction under nitrogen. Condensation between $[\text{Fe}_3(\text{CO})_{11}\text{H}]^-$ and $\text{Ni}(\text{CO})_4$ has not been observed even in the presence of a strong excess of $\text{Ni}(\text{CO})_4$ and under UV radiation. This last behavior is probably the consequence of the reduced free negative charge of the starting $[\text{Fe}_3(\text{CO})_{11}\text{H}]^-$. When reacting $\text{Ni}(\text{CO})_4$ with more reduced iron carbonyl anions such as $[\text{Fe}_2(\text{CO})_8]^{2-}$ or $[\text{Fe}(\text{CO})_4]^{2-}$, we have spectroscopic evidence of the formation of mixed Fe-Ni carbonyl anionic species other than $[\text{Fe}_3\text{Ni}(\text{CO})_{12}]^{2-}$. However, only the latter species has thus far been isolated from these reactions, probably owing to rearrangements during the workup of the solutions.

The formation of $[\text{Fe}_3\text{Ni}(\text{CO})_{12}]^{2-}$ appears to be so favored that it has also been isolated from reaction of a reduced nickel

(13) The $[\text{Fe}_3(\text{CO})_{11}\text{H}]^-$ monoanion is degraded by carbon monoxide (1 atm) to a mixture of $[\text{Fe}(\text{CO})_4\text{H}]^-$ and $\text{Fe}(\text{CO})_5$, only at higher temperature (ca. 60 °C).

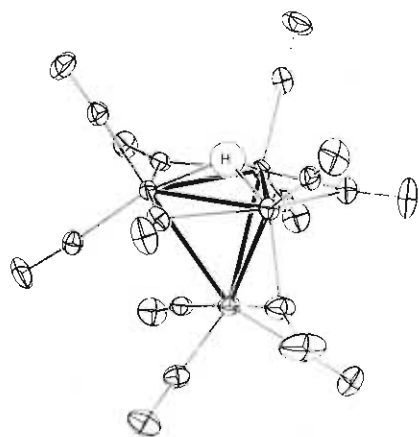


Figure 1. Perspective view of the $[\text{Fe}_3\text{Ni}(\text{CO})_{12}\text{H}]^-$ anion, with thermal ellipsoids drawn to enclose 20% probability.¹⁸

carbonyl anion such as $[\text{Ni}_5(\text{CO})_{12}]^{2-}$ with an excess of a zerovalent iron carbonyl species, e.g. $\text{Fe}(\text{CO})_5$.

Both $[\text{Fe}_3\text{Ni}(\text{CO})_{12}]^{2-}$ and $[\text{Fe}_3\text{Ni}(\text{CO})_{12}\text{H}]^-$ also have been synthesized by reaction of $[\text{Fe}_3(\text{CO})_{11}]^{2-}$ with an ethanol solution of $\text{NiCl}_2 \cdot x\text{EtOH}$. When the $\text{NiCl}_2 \cdot x\text{EtOH}$ solution is added through a microburet, IR monitoring of the reaction shows the formation of fairly pure $[\text{Fe}_3\text{Ni}(\text{CO})_{12}]^{2-}$ as the molar ratio between the two reagents approaches ca. 1:1. The apparent stoichiometry (5) accounts for this approximate molar ratio, and it is in fair agreement with the amount of Fe^{2+} found in solution at the end of the reaction. Reaction 5 is



complicated by the formation of some $\text{Fe}(\text{CO})_5$ and $\text{Ni}(\text{CO})_4$, probably arising from a degradation reaction due to evolving carbon monoxide, such as those represented by the back-reaction of equilibrium 1 and the forward reaction of equilibrium 2. $[\text{Fe}_3\text{Ni}(\text{CO})_{12}]^{2-}$ is also the first detectable product upon reaction of $[\text{Fe}_2(\text{CO})_8]^{2-}$ with $\text{NiCl}_2 \cdot x\text{EtOH}$. In both reactions, upon addition of excess $\text{NiCl}_2 \cdot x\text{EtOH}$ solution, the $[\text{Fe}_3\text{Ni}(\text{CO})_{12}]^{2-}$ dianion is converted into the corresponding $[\text{Fe}_3\text{Ni}(\text{CO})_{12}\text{H}]^-$ anion, probably due to the acidity of the $\text{NiCl}_2 \cdot x\text{EtOH}$ solution. Since too large an excess of Ni(II) salts results in complete decomposition, it is necessary to precipitate the $[\text{Fe}_3\text{Ni}(\text{CO})_{12}\text{H}]^-$ monoanion by addition of excess cation as soon as IR monitoring shows complete conversion. Alternatively, the protonation step may be accomplished by adding H_3PO_4 or acetic acid in ethanol.

Crystal Structure of $[\text{N}(\text{CH}_3)_3\text{CH}_2\text{Ph}][\text{Fe}_3\text{Ni}(\text{CO})_{12}\text{H}]^-$. The X-ray structure of $[\text{N}(\text{CH}_3)_3\text{CH}_2\text{Ph}][\text{Fe}_3\text{Ni}(\text{CO})_{12}\text{H}]^-$ consists of discrete cations and anions packed in general positions in a triclinic cell of space group $P\bar{1}$. A drawing of the $[\text{Fe}_3\text{Ni}(\text{CO})_{12}\text{H}]^-$ monoanion with thermal ellipsoids is shown in Figure 1, and a sketch indicating the numbering of the atoms is given in Figure 2. Despite the absence of any crystallographic symmetry, an approximate mirror plane may be recognized comprising the atoms Ni, Fe(3), and H and bisecting the Fe(1)–Fe(2) bond. The idealized symmetry of the anion may therefore be assumed to be C_s . The most significant bond distances and angles for the $[\text{Fe}_3\text{Ni}(\text{CO})_{12}\text{H}]^-$ anion are reported in Tables III and IV (bonding parameters for the $[\text{N}(\text{CH}_3)_3\text{CH}_2\text{Ph}]^+$ cation all fall within the normal range and have been included in supplementary Tables II-S and III-S). The metal–metal distances in the tetrahedral metal core of the anion are scattered in the range 2.47–2.72 Å, with the shortest distances being associated with the unique nickel atom ($\text{Ni}-\text{Fe}_{\text{av}} = 2.50$ Å). The unique Fe(1)–Fe(2) bond in the Fe_2Ni basal plane (2.570 (2) Å) is significantly shorter than the two unbridged Fe–Fe bonds connecting the apical iron

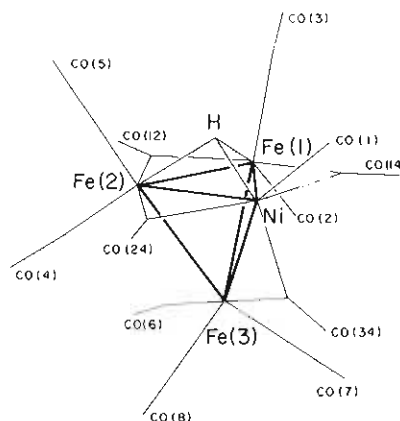


Figure 2. Schematic drawing of the anion showing the atom-numbering scheme.

Table III. Bond Distances (Å) in the $[\text{Fe}_3\text{Ni}(\text{CO})_{12}\text{H}]^-$ Anion

M–M			
Ni–Fe(1)	2.4712 (8)	Fe(1)–Fe(2)	2.570 (2)
Ni–Fe(2)	2.5047 (6)	Fe(1)–Fe(3)	2.720 (1)
Ni–Fe(3)	2.5252 (7)	Fe(2)–Fe(3)	2.7139 (9)
M–C(terminal)			
Ni–C(1)	1.763 (3)	Fe(2)–C(5)	1.776 (2)
Fe(1)–C(2)	1.766 (2)	Fe(3)–C(6)	1.791 (3)
Fe(1)–C(3)	1.777 (3)	Fe(3)–C(7)	1.774 (2)
Fe(2)–C(4)	1.773 (2)	Fe(3)–C(8)	1.791 (3)
M–C(bridge)			
Ni–C(14)	2.157 (2)	Fe(1)–C(14)	1.853 (3)
Ni–C(24)	2.232 (2)	Fe(2)–C(12)	1.980 (2)
Ni–C(34)	1.869 (3)	Fe(2)–C(24)	1.838 (2)
Fe(1)–C(12)	1.981 (2)	Fe(3)–C(34)	2.002 (3)
M–H			
Ni–H	1.55 (3)	Fe(2)–H	1.61 (3)
Fe(1)–H	1.56 (2)		
C=O(terminal)			
O(1)–C(1)	1.121 (3)	O(5)–C(5)	1.134 (3)
O(2)–C(2)	1.146 (2)	O(6)–C(6)	1.145 (3)
O(3)–C(3)	1.137 (3)	O(7)–C(7)	1.142 (3)
O(4)–C(4)	1.141 (3)	O(8)–C(8)	1.143 (3)
C=O(bridge)			
O(12)–C(12)	1.173 (3)	O(24)–C(24)	1.158 (3)
O(14)–C(14)	1.163 (3)	O(34)–C(34)	1.156 (4)

atom Fe(3) with the basal plane (mean distance 2.717 (3) Å).

Eight of the twelve carbonyl groups are terminally bonded with one, two, two, and three groups bound to Ni, Fe(1), Fe(2), and Fe(3), respectively ($\text{M}-\text{C}_{\text{av}} = 1.78$, $\text{C}-\text{O}_{\text{av}} = 1.14$ Å). Three bridging carbonyl groups span the edges of the basal triangular face bridged by the hydride ligand and are almost coplanar with the trimetal ring. While the carbonyl group bridging the Fe(1)–Fe(2) bond is symmetrical, the remaining two are unsymmetrically bridging the Fe–Ni bonds ($\text{Fe}-\text{C}_{\text{av}} = 1.85$, $\text{Ni}-\text{C}_{\text{av}} = 2.19$, $\text{C}-\text{O}_{\text{av}} = 1.16$ Å). The fourth bridging carbonyl group lies on the approximate mirror plane and spans the edge connecting the nickel atom with the apical Fe(3). This group is also unsymmetrical but has its shortest contact with the nickel atom ($\text{Fe}-\text{C} = 2.00$, $\text{Ni}-\text{C} = 1.87$, $\text{C}-\text{O} = 1.16$ Å).

The hydride ligand has been located directly from X-ray data in the final difference Fourier maps and refined isotopically. Its stereochemistry is depicted in Figure 3. The distance of 0.60 (3) Å from the Fe_2Ni basal plane, as well as the average M–H bond distance of 1.57 Å, is rather short when compared with typically more accurate M–H bond distances derived from neutron diffraction studies. For instance, the face-bridging hydride atoms in $\text{HCo}_3\text{Fe}(\text{CO})_9(\text{P}(\text{OME})_3)_3$ and $\text{H}_3\text{Ni}_4(\eta^5-\text{C}_5\text{H}_5)_4$ have been found at ca. 0.90 Å from the trimetal rings and show Co–H and Ni–H bond distances of

Table IV. Bond Angles (Deg) in the $[\text{Fe}_3\text{Ni}(\text{CO})_{12}\text{H}]^-$ Anion

M-M-M			
Fe(1)-Ni-Fe(2)	62.19 (4)	Ni-Fe(2)-Fe(1)	58.27 (2)
Fe(1)-Ni-Fe(3)	65.94 (4)	Ni-Fe(2)-Fe(3)	57.71 (2)
Fe(2)-Ni-Fe(3)	65.31 (3)	Fe(1)-Fe(2)-Fe(3)	61.88 (4)
Ni-Fe(1)-Fe(2)	59.55 (3)	Ni-Fe(3)-Fe(1)	56.08 (3)
Ni-Fe(1)-Fe(3)	57.98 (2)	Ni-Fe(3)-Fe(2)	56.98 (2)
Fe(2)-Fe(1)-Fe(3)	61.66 (3)	Fe(1)-Fe(3)-Fe(2)	56.46 (4)
M-M-C(terminal)			
Fe(1)-Ni-C(1)	136.13 (8)	Ni-Fe(2)-C(5)	120.41 (9)
Fe(2)-Ni-C(1)	132.98 (7)	Fe(1)-Fe(2)-C(5)	116.51 (8)
Fe(3)-Ni-C(1)	153.64 (9)	Fe(3)-Fe(2)-C(5)	177.89 (8)
Ni-Fe(1)-C(2)	139.99 (9)	Ni-Fe(3)-C(6)	134.39 (8)
Fe(2)-Fe(1)-C(2)	129.76 (8)	Fe(1)-Fe(3)-C(6)	82.81 (8)
Fe(3)-Fe(1)-C(2)	90.55 (8)	Fe(2)-Fe(3)-C(6)	85.35 (8)
Ni-Fe(1)-C(3)	117.78 (8)	Ni-Fe(3)-C(7)	110.85 (9)
Fe(2)-Fe(1)-C(3)	116.21 (7)	Fe(1)-Fe(3)-C(7)	99.14 (9)
Fe(3)-Fe(1)-C(3)	175.71 (7)	Fe(2)-Fe(3)-C(7)	155.58 (9)
Ni-Fe(2)-C(4)	137.54 (8)	Ni-Fe(3)-C(8)	116.67 (8)
Fe(1)-Fe(2)-C(4)	128.99 (6)	Fe(1)-Fe(3)-C(8)	156.98 (7)
Fe(3)-Fe(2)-C(4)	87.60 (7)	Fe(2)-Fe(3)-C(8)	100.73 (8)
M-M-C(bridge)			
Fe(1)-Ni-C(14)	46.59 (7)	Fe(2)-Fe(1)-C(14)	117.20 (7)
Fe(1)-Ni-C(24)	107.40 (8)	Fe(3)-Fe(1)-C(12)	86.23 (8)
Fe(1)-Ni-C(34)	112.47 (8)	Fe(3)-Fe(1)-C(14)	82.99 (9)
Fe(2)-Ni-C(14)	108.71 (7)	Ni-Fe(2)-C(12)	107.82 (8)
Fe(2)-Ni-C(24)	45.22 (7)	Ni-Fe(2)-C(24)	59.53 (8)
Fe(2)-Ni-C(34)	105.8 (1)	Fe(1)-Fe(2)-C(12)	49.56 (7)
Fe(3)-Ni-C(14)	82.46 (8)	Fe(1)-Fe(2)-C(24)	117.79 (8)
Fe(3)-Ni-C(24)	83.08 (7)	Fe(3)-Fe(2)-C(12)	86.40 (8)
Fe(3)-Ni-C(34)	51.60 (9)	Fe(3)-Fe(2)-C(24)	85.73 (8)
Ni-Fe(1)-C(12)	109.08 (7)	Ni-Fe(3)-C(34)	47.02 (9)
Ni-Fe(1)-C(14)	57.73 (7)	Fe(1)-Fe(3)-C(34)	99.12 (9)
Fe(2)-Fe(1)-C(12)	49.54 (6)	Fe(2)-Fe(3)-C(34)	94.97 (8)
M-M-H			
Fe(1)-Ni-H	37.6 (7)	Fe(3)-Fe(1)-H	77 (1)
Fe(2)-Ni-H	38 (1)	Ni-Fe(2)-H	37 (1)
Fe(3)-Ni-H	84 (1)	Fe(1)-Fe(2)-H	35.2 (8)
Ni-Fe(1)-H	37 (1)	Fe(3)-Fe(2)-H	76.9 (9)
Fe(2)-Fe(1)-H	36 (1)		
C-M-C			
C(1)-Ni-C(14)	103.7 (1)	C(4)-Fe(2)-C(5)	94.5 (1)
C(1)-Ni-C(24)	98.92 (9)	C(4)-Fe(2)-C(12)	92.0 (1)
C(1)-Ni-C(34)	102.0 (1)	C(4)-Fe(2)-C(24)	97.6 (1)
C(14)-Ni-C(24)	153.9 (1)	C(5)-Fe(2)-C(12)	93.4 (1)
C(14)-Ni-C(34)	98.4 (1)	C(5)-Fe(2)-C(24)	94.1 (1)
C(24)-Ni-C(34)	89.4 (1)	C(12)-Fe(2)-C(24)	167.33 (9)
C(2)-Fe(1)-C(3)	93.5 (1)	C(6)-Fe(3)-C(7)	92.9 (1)
C(2)-Fe(1)-C(12)	90.9 (1)	C(6)-Fe(3)-C(8)	93.0 (1)
C(2)-Fe(1)-C(14)	97.7 (1)	C(6)-Fe(3)-C(34)	177.9 (1)
C(3)-Fe(1)-C(12)	95.0 (1)	C(7)-Fe(3)-C(8)	103.7 (1)
C(3)-Fe(1)-C(14)	95.2 (1)	C(7)-Fe(3)-C(34)	87.7 (1)
C(12)-Fe(1)-C(14)	166.24 (9)	C(8)-Fe(3)-C(34)	84.9 (1)
C-M-H			
C(1)-Ni-H	122 (1)	C(12)-Fe(1)-H	80 (1)
C(14)-Ni-H	79.2 (8)	C(14)-Fe(1)-H	89 (1)
C(24)-Ni-H	77.7 (8)	C(4)-Fe(2)-H	162.4 (8)
C(34)-Ni-H	135 (1)	C(5)-Fe(2)-H	101.0 (9)
C(2)-Fe(1)-H	165 (1)	C(12)-Fe(2)-H	79.0 (9)
C(3)-Fe(1)-H	99 (1)	C(24)-Fe(2)-H	89.6 (9)
M-C=O(terminal)			
Ni-C(1)-O(1)	177.1 (2)	Fe(2)-C(5)-O(5)	176.9 (2)
Fe(1)-C(2)-O(2)	177.1 (2)	Fe(3)-C(6)-O(6)	174.8 (2)
Fe(1)-C(3)-O(3)	178.2 (2)	Fe(3)-C(7)-O(7)	179.0 (2)
		Fe(3)-C(8)-O(8)	178.5 (2)
M-C=O(bridge)			
Fe(1)-C(12)-O(12)	139.8 (1)	Ni-C(24)-O(24)	123.8 (2)
Fe(2)-C(12)-O(12)	139.2 (1)	Fe(2)-C(24)-O(24)	160.9 (2)
Ni-C(14)-O(14)	125.9 (2)	Ni-C(34)-O(34)	136.1 (2)
Fe(1)-C(14)-O(14)	158.4 (2)	Fe(3)-C(34)-O(34)	142.4 (2)
M-C-M(bridge)			
Fe(1)-C(12)-Fe(2)	80.9 (1)	Ni-C(24)-Fe(2)	75.26 (8)
Ni-C(14)-Fe(1)	75.68 (8)	Ni-C(34)-Fe(3)	81.4 (1)
M-H-M			
Ni-H-Fe(1)	105 (1)	Fe(1)-H-Fe(2)	108 (2)
Ni-H-Fe(2)	105 (2)		

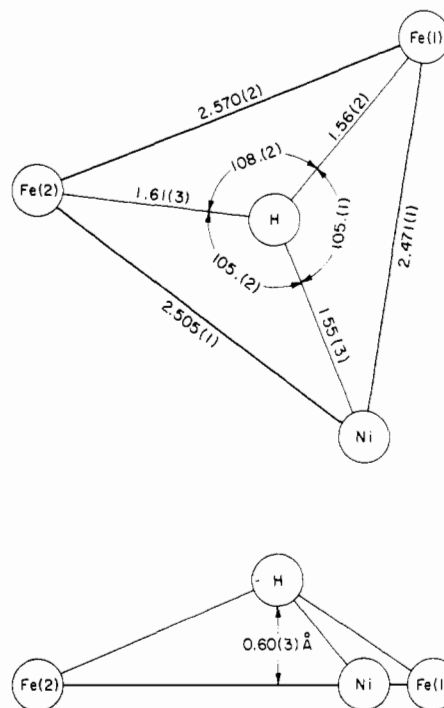


Figure 3. Environment of the hydrogen atom.

1.73 and 1.69 Å, respectively.^{14,15} However, this discrepancy is to be expected and reflects the relatively lower accuracies and systematic errors generally associated with X-ray-determined M-H bond distances.

The apparently complicated stereochemistry of the $[\text{Fe}_3\text{Ni}(\text{CO})_{12}\text{H}]^-$ monoanion, as reflected by its low idealized C_3 symmetry, probably arises from both steric and electronic requirements. From one point of view, a distorted icosahedral packing of 12 carbonyl groups, such as found in this cluster, appears to be the most favored for tetrahedral clusters of metals of the first transition series.¹⁶ The overall structure of $[\text{Fe}_3\text{Ni}(\text{CO})_8(\mu\text{-CO})_4(\mu_3\text{-H})]^-$ may be related, for instance, to that of the $[\text{Fe}_4(\text{CO})_9(\mu\text{-CO})_3(\mu_3\text{-CO})]^{2-}$ dianion,¹⁷ by replacing the face-bridging hydride ligand in the former with a face-bridging carbonyl group and by bringing into a terminal position the unsymmetrically bridging carbonyl group spanning the Ni-Fe(3) edge. On the other hand, following a noble-gas formalism, the presently observed orientation of the bimetallic tetrahedral core comprised of a unique electron-rich nickel and three iron atoms with respect to the icosahedral packing of carbonyl ligands allows equalization of the electron distribution onto the different metal centers.

Concluding Remarks

The solid-state structure found for $[\text{Fe}_3\text{Ni}(\text{CO})_{12}\text{H}]^-$ may also be retained in solution as shown by the fact that the IR spectrum shows a complicated pattern, particularly in the edge-bridging carbonyl region. On this basis it is also likely that the parent $[\text{Fe}_3\text{Ni}(\text{CO})_{12}]^{2-}$ dianion, which shows a closely related pattern, may possess an analogous structure.

The synthesis of tetranuclear species by reaction 5 may be contrasted with the isolation of pentanuclear $[\text{Fe}_4\text{M}(\text{CO})_{16}]^{2-}$ (M = Pd, Pt) clusters, recalling square-planar complexes of Pd(II) and Pt(II) when either $[\text{Fe}_3(\text{CO})_{11}]^{2-}$ or $[\text{Fe}_2(\text{CO})_8]^{2-}$ is reacted with palladium or platinum dichloride.⁶ Corre-

(14) Teller, R. G.; Wilson, R. D.; McMullan, R. K.; Koetzle, T. F.; Bau, R. *J. Am. Chem. Soc.* **1978**, *100*, 3071.

(15) Koetzle, T. F.; Müller, J.; Tipton, D. L.; Hart, D. W.; Bau, R. *J. Am. Chem. Soc.* **1979**, *101*, 5631.

(16) Chini, P.; Heaton, B. T. *Top. Curr. Chem.* **1977**, *71*, 1.

(17) Doedens, R. J.; Dahl, L. F. *J. Am. Chem. Soc.* **1966**, *88*, 4847.

(18) Johnson, C. K. "ORTEP II", Report ORNL-5138; Oak Ridge National Laboratory: Oak Ridge, TN, 1976.

spondingly, in all the reactions investigated there also has been no spectroscopic evidence of the existence of species such as $[\text{Fe}_3\text{Pt}_3(\text{CO})_{15}]^{2-}$.⁷ This further difference in the carbonyl cluster chemistry of nickel subgroup metals is well in keeping with the tendency to square-planar coordination of both palladium and platinum and with their aversion to high coordination number with CO, contrasted to the preference of nickel for tetrahedral coordination and the stability of $\text{Ni}(\text{C}-\text{O})_4$.

Acknowledgment. The research at Brookhaven National Laboratory was carried out under contract with the U.S. Department of Energy and supported by its Office of Basic Energy Sciences.

Registry No. $[\text{N}(\text{CH}_3)_3\text{CH}_2\text{Ph}][\text{Fe}_3\text{Ni}(\text{CO})_{12}\text{H}]$, 89322-11-2; $[\text{PPh}_3(\text{CH}_2\text{Ph})]_2[\text{Fe}_3\text{Ni}(\text{CO})_{12}]$, 89322-13-4; $[\text{PPh}_3(\text{CH}_2\text{Ph})]_2[\text{Fe}_3(\text{CO})_{11}]$, 89322-14-5; $\text{Ni}(\text{CO})_4$, 13463-39-3; $[\text{N}(\text{C}_4\text{H}_9)_4]_2[\text{Fe}_3\text{Ni}(\text{C}-\text{O})_{12}]$, 89322-15-6; $[\text{N}(\text{CH}_3)_3\text{CH}_2\text{Ph}]_2[\text{Fe}_3\text{Ni}(\text{CO})_{12}]$, 89322-16-7; $[\text{PPh}_3(\text{CH}_2\text{Ph})][\text{Fe}_3\text{Ni}(\text{CO})_{12}\text{H}]$, 89322-17-8; $[\text{N}(\text{C}_4\text{H}_9)_4][\text{Fe}_3\text{Ni}(\text{CO})_{12}\text{H}]$, 89322-18-9; $[\text{PPN}][\text{Fe}_3\text{Ni}(\text{CO})_{12}\text{H}]$, 89322-19-0; $[\text{N}(\text{C}_4\text{H}_9)_4]_2[\text{Fe}_3(\text{CO})_{11}]$, 89322-20-3; $[\text{N}(\text{C}_4\text{H}_9)_4]_2[\text{Fe}_2(\text{CO})_8]$, 58341-98-3; $[\text{Fe}_3(\text{CO})_{11}\text{H}]^-$, 55188-22-2; $[\text{Na}(\text{THF})_4]_2[\text{Fe}(\text{CO})_4]$, 89322-21-4; Fe, 7439-89-6; Ni, 7440-02-0.

Supplementary Material Available: Thermal parameters (Table I-S), bond distances (Table II-S) and angles (Table III-S) in the $[\text{N}(\text{CH}_3)_3\text{CH}_2\text{Ph}]^+$ cation, and a listing of observed and calculated F^2 values (26 pages). Ordering information is given on any current masthead page.

Contribution from the Department of Chemistry,
Texas Christian University, Fort Worth, Texas 76129

Synthesis and Stereochemistry of Some Alkyl[bis(trimethylsilyl)amino]boranes

BEI-LI LI, MARY A. GOODMAN, and ROBERT H. NEILSON*

Received July 20, 1983

Several new alkylchloro- and alkyl(dimethylamino)[bis(trimethylsilyl)amino]boranes, $(\text{Me}_3\text{Si})_2\text{NB}(\text{R})\text{X}$ [$\text{X} = \text{Cl}$ ($\text{R} = t\text{-Bu}$, $i\text{-Pr}$, CH_2SiMe_3); $\text{X} = t\text{-Bu}$ ($\text{R} = \text{CH}_2\text{SiMe}_3$); $\text{X} = \text{NMe}_2$ ($\text{R} = \text{Me}$, CH_2SiMe_3 , $i\text{-Pr}$, $t\text{-Bu}$)], have been prepared from $(\text{Me}_3\text{Si})_2\text{NBCl}_2$ by chloride displacement with organometallic reagents and $\text{Me}_3\text{SiNMe}_2$. Rotational barriers ($\Delta G_c^\ddagger = 17.3\text{--}20.9$ kcal/mol) about the B-NMe₂ bonds were determined by dynamic ¹H NMR spectroscopy, and the results are discussed in terms of steric interactions between the bulky groups on boron. Analogies between the preparative chemistry of these (silylamino)boranes and that of the comparably substituted phosphines are noted.

Introduction

The chemistry and stereochemistry of compounds containing the silicon-nitrogen-boron linkage have been the subjects of numerous studies during the past two decades. Many of these compounds are, in fact, useful precursors to other B-N systems including diborylamines,¹ borazines,² borazocines,³ monomeric boron imines,⁴ and B-H-substituted aminoboranes.⁵ Recent interest in our laboratory has focused mainly on the synthetic potential of analogous silicon-nitrogen-phosphorus compounds.⁶ Clearly, there exist many parallels between the preparative chemistry of (silylamino)boranes and that of the (silylamino)phosphines [e.g., $(\text{Me}_3\text{Si})_2\text{NBCl}_2$, $(\text{Me}_3\text{Si})_2\text{NP}(\text{Cl})_2$]. We are beginning to explore the extent of this analogy in more detail toward the goal of developing new synthetic methods and reactivity patterns in B-N chemistry.

From a stereochemical viewpoint, interest in (silylamino)boranes was stimulated by Wells and co-workers,⁷ who observed an unexpectedly high barrier to rotation ($\Delta G^\ddagger = 17.6$

kcal/mol) about the $\text{Me}_2\text{N-B}$ bond in $(\text{Me}_3\text{Si})_2\text{NB}(\text{Cl})\text{NMe}_2$. Subsequent studies⁸⁻¹⁰ on related compounds led to the conclusion that the bulky $(\text{Me}_3\text{Si})_2\text{N}$ group is rotated out of the plane of the B-NMe₂ moiety and thus is not an effective π donor to boron (Figure 1A). The same type of conformation has been recently postulated¹¹ for the sterically congested (tetramethylpiperidino)boranes (Figure 1B). The previous dynamic NMR studies of (silylamino)boranes $\text{R}_2\text{SiN}(\text{R})\text{B}(\text{X})\text{NR}_2$ have probed the effects of varying substituents on silicon¹⁰ as well as on both of the nitrogen atoms.^{8,9} For synthetic simplicity, however, the other substituents on boron have been largely restricted to $\text{X} = \text{phenyl}$ and, in a few cases, to $\text{X} = \text{Cl}$ or NH_2 . The stereochemical influence of groups (e.g., $\text{X} = \text{alkyl}$) that may be varied in size and are not π donors to boron has not been investigated.

In the context of these preparative and stereochemical questions, we report here on the synthesis, reactivity, and dynamic NMR study of several new B-alkylated (silylamino)boranes.

Results and Discussion

Synthesis. We have previously reported that bulky organometallic reagents (e.g., $t\text{-BuLi}$, $\text{Me}_3\text{SiCH}_2\text{MgCl}$, $i\text{-PrMgCl}$) react with [bis(trimethylsilyl)amino]dichlorophosphine to yield the monosubstituted alkylchlorophosphines $(\text{Me}_3\text{Si})_2\text{NP}(\text{R})\text{Cl}$.^{12,13} In the present study, we find that the

- (a) Nöth, H.; Storch, W. *Chem. Ber.* **1976**, *109*, 884. (b) Barlos, K.; Christl, H.; Nöth, H. *Justus Liebig's Ann. Chem.* **1976**, 2272.
- Bowser, J. R.; Neilson, R. H.; Wells, R. L. *Inorg. Chem.* **1978**, *17*, 1882.
- Neilson, R. H.; Wells, R. L. *Synth. Inorg. Met.-Org. Chem.* **1973**, *3*, 283.
- Paetzold, P.; von Plotho, C. *Chem. Ber.* **1982**, *115*, 2819 (and references cited therein).
- (a) Nutt, W. R.; Wells, R. L. *Inorg. Chem.* **1982**, *21*, 2473. (b) Wisian-Neilson, P.; Martin, D. R. *J. Inorg. Nucl. Chem.* **1979**, *41*, 1545. (c) Neilson, R. H. *Inorg. Chem.* **1980**, *19*, 755.
- See, for example, the following and references cited therein: (a) Li, B.-L.; Engenito, J. S.; Neilson, R. H.; Wisian-Neilson, P. *Inorg. Chem.* **1983**, *22*, 575. (b) Neilson, R. H.; Engenito, J. S. *Organometallics* **1982**, *1*, 1270. (c) Neilson, R. H.; Wisian-Neilson, P. *Inorg. Chem.* **1982**, *21*, 3568.
- Wells, R. L.; Paige, H. L.; Moreland, C. G. *Inorg. Nucl. Chem. Lett.* **1971**, *7*, 177.

- Neilson, R. H.; Wells, R. L. *Inorg. Chem.* **1977**, *16*, 7.
- Graham, D. M.; Bowser, J. R.; Moreland, C. G.; Neilson, R. H.; Wells, R. L. *Inorg. Chem.* **1978**, *17*, 2028.
- Beswick, Y. F.; Wisian-Neilson, P.; Neilson, R. H. *J. Inorg. Nucl. Chem.* **1981**, *43*, 2639.
- Nöth, H.; Staudigl, R.; Wagner, H.-U. *Inorg. Chem.* **1982**, *21*, 706.
- Neilson, R. H. *Inorg. Chem.* **1981**, *20*, 1679.
- O'Neal, H. R.; Neilson, R. H. *Inorg. Chem.* **1983**, *22*, 814.